HHS Public Access

Author manuscript

Prostate. Author manuscript; available in PMC 2016 February 01.

Published in final edited form as:

Prostate. 2016 February ; 76(2): 215–225. doi:10.1002/pros.23115.

Characterization of a Novel Metastatic Prostate Cancer Cell Line of LNCaP Origin

Mark A. Castanares[1,†], **Ben T. Copeland**[2,†], **Wasim H. Chowdhury**[3], **Minzhi M. Liu**[3], **Ronald Rodriguez**[3], **Martin G. Pomper**[2], **Shawn E. Lupold**[3], and **Catherine A. Foss**[2,*]

[1]Department of Pharmacology and Molecular Sciences, Lilly Corporate Center, Indianapolis, Indiana [2]Russell H Morgan Department of Radiology and Radiological Sciences, Johns Hopkins University School of Medicine, Baltimore, Maryland [3]The James Buchanan Brady Urologic Institute and Department of Urology, Johns Hopkins School of Medicine, Baltimore, Maryland

Abstract

Background—The LNCaP cell line was originally isolated from the lymph node of a patient with metastatic prostate cancer. Many cell lines have been derived from LNCaP by selective pressures to study different aspects of prostate cancer progression. When injected subcutaneously into male athymic nude mice, LNCaP and its derivatives rarely metastasize.

Methods—Here, we describe the characteristics of a new LNCaP derivative, JHU-LNCaPSM, which was generated by long term passage in normal cell culture conditions.

Results—Short tandem repeat (STR) analysis and genomic sequencing verified JHU-LNCaP-SM derivation from parental LNCaP cells. JHU-LNCaP-SM cells express the same mutated androgen receptor (AR) but unlike LNCaP, are no longer androgen dependent for growth. The cells demonstrate an attenuated androgen responsiveness in transcriptional assays and retain androgen sensitive expression of PSA, AR, and PSMA. Unlike parental LNCaP, JHU-LNCaP-SM cells quickly form subcutaneous tumors in male athymic nude mice, reliably metastasize to the lymph nodes and display a striking intra-tumoral and spreading hemorrhagic phenotype as tumor xenografts.

Conclusions—The JHU-LNCaP-SM cell line is a new isolate of LNCaP, which facilitates practical, preclinical studies of spontaneous metastasis of prostate cancer through lymphatic tissues.

Keywords

JHU-LNCaP-SM; PSMA; metastasis; androgen; lymph node

[*]Correspondence to: Catherine A. Foss, Russell H Morgan Department of Radiology and Radiological Sciences, CRB2 493, Johns Hopkins University School of Medicine, Baltimore, MD, 21228. cfoss1@jhmi.edu.

[†]Mark A. Castanares and Ben T. Copeland contributed equally to this work.

Current address of Mark A. Castanares: Lilly Corporate Center., Indianapolis, Indiana.

Current address of Wasim H. Chowdhury and Ronald Rodriguez: University of Texas, San Antonio.

Disclosures: There are no affiliations or conflicts to disclose.

Supporting Information: Additional supporting information may be found in the online version of this article at the publisher's web-site.

Introduction

Pre-clinical prostate cancer research is currently limited by the number and characteristics of existing cell lines used to study the disease. There is a deficiency of cell lines which accurately recapitulate the disease progression of human prostate cancer. LNCaP is a cell line derived from a metastatic lymph node lesion of human prostate cancer which is androgen receptor (AR) positive, exhibits androgen-sensitive growth, and was originally reported by Horoszewicz et al. to form subcutaneous tumors in intact male athymic nude mice at a frequency of 58% [1,2].

Many LNCaP sublines have been derived by long-term culture of LNCaP cells in steroid-free media or serial passage in castrated hosts to generate cells which no longer display androgen-sensitive growth [3–8]. Others have observed that LNCaP cells gradually lose their androgen-sensitive growth characteristic upon continuous passage (>80) [9,10]. This suggests that simple passage of LNCaP cells can facilitate one aspect of natural prostate cancer progression from an androgen-dependent to an andro-gen-independent state.

There are very few well characterized models to pre-clinically study prostate cancer in vivo that recapitulate the full extent of the human disease, including reliable spontaneous, distant metastases [11,12]. Subcutaneous and orthotopic xenografts of human cell lines implanted into athymic nude mice are the standard method to study the biology of prostate cancer. However, some cell lines do not grow well in vivo and may take long periods of time to establish tumors. Orthotopic implantation of cancer cells is a common route to study the biology of prostate cancer and can reliably generate lymph node and other metastasis after a few months [13]. However, orthotopic injections are cumbersome, primary and secondary disease progression may be difficult to monitor and the primary tumor typically kills the host by way of urinary obstruction prior to establishment of observable metastatic disease. Very few cell lines will metastasize after subcutaneous tumor formation, making it difficult to readily study the metastatic process. Subcutaneous placement of cells to form a primary tumor allows for convenient monitoring of the primary tumor, placement away from internal tissues and it permits subsequent, simple resection of the primary tumor to allow long term development of any secondary disease. This route also enables metastasis to proceed spontaneously as opposed to a random deposition from intravenous and intracardiac injection of cells.

The Prostate Specific Membrane Antigen (PSMA) is a biomarker for advanced PCa that is upregulated in primary prostate tumors, contrasted with normal prostate epithelium and most abundantly expressed in advanced metastatic and hormone refractory PCa [14,15]. Unlike PSA, PSMA expression reliably increases following androgen ablation [14,16]. Therefore, PSMA has become a rapidly expanding target for imaging and therapy in both pre-clinical and clinical settings and has been the target of several FDA approved imaging agents [17–25]. None of the available genetically engineered murine models of spontaneous prostate cancer form tumors that express PSMA, which is a substantial deficiency of these models, also making them unsuitable for evaluation of emerging PSMA-targeted diagnostics and therapeutics. Any pre-clinical model of prostate cancer seeking to replicate advanced

androgen-insensitive prostate cancer, including the ability to spontaneously metastasize from a parental tumor, should express PSMA since 72% of clinical lymph node and 92% of bone metastases express PSMA [26].

Here we describe a novel LNCaP subline, JHU-LNCaP-SM, which was obtained by long term serial passaging in standard growth medium, that displays androgen-insensitive growth, readily forms subcutaneous tumors, reliably metastasizes to the lymph nodes in athymic nude mice and retains androgen-responsive expression of PSMA.

Materials and Methods

Cell Lines

LNCaP and C4-2 cells were obtained from the American Type Tissue Collection (ATCC) (Rockville, MD). Cells were grown in RPMI 1640 media (Corning, Manassas, VA) containing either 10% fetal bovine serum (Gemini Bio-Products, West Sacramento, CA) or 10% charcoal stripped fetal bovine serum (HyClone, Logan, UT and Sigma, St. Louis, MO) and supplemented with Ciprofloxacin Hydrochloride 5μg/ml (US Biological, Swampscott, MA), and Gentamicin 50 μg/ml (Quality Biological Inc., Gaithersburg, MD). The cells were passaged in uncoated filter top polystyrene flasks (Corning) and were maintained at 37°C in 5% CO_2 in humidified air. Cells were typically split at 80% confluency using 0.05% trypsin (cat # 25-052-CI; Corning) in calcium-free Hank's Buffered Salt Solution (Corning).

Short Tandem Repeat Profiling

Genomic DNA was collected from LNCaP, C4-2 and JHU-LNCaP-SM using the DNA Easy Blood and Tissue kit (Qiagen, Valencia, CA) according to the manufacture's protocol. Genomic DNA was analyzed using the PowerPlex 1.2 system (Promega, Madison, WI) on an Applied Biosystem 3730XL genetic analyzer by the Fragment Analysis Facility at Johns Hopkins University. STR profiles were compared using the DSMZ database for known cell line reference profiles (http://www.dsmz.de/services/services-human-and-animal-cell-lines/online-str-analysis.html).

Androgen Receptor Mutation Sequencing

Genomic DNA was collected from LNCaP, C4-2, and JHU-LNCaP-SM using the DNA Easy Blood and Tissue kit (Qiagen) according to the manufacture's protocol. A fragment containing codon 877 of the AR was amplified by PCR using primers for AR region H by Lubahn et al. [27] (AR-H F: GAGGC-CACCTCCTTGTCAACCCTG, AR-H R: GAA-CATGTTCATGACAGACTGTACATCA) using GoTaq Green Master Mix (Promega) according to manufacturer's protocol. PCR products were sequenced at the JHMI Synthesis and Sequencing Facility using an Applied Biosystems 3730XL DNA Analyzer. Sequencing data was analyzed using Vector NTI 9 software (Invitrogen, Carlsbad, CA).

Luciferase Reporter Assay

Confluent T75 flasks were transfected with 10μg of pBk-PSE-PBN-Luc and 1μg pRL-CMV using Lipofectamine Plus Reagent (Invitrogen) as per the manufacturer's protocol. Eight hours after transfection, cells were harvested and plated in a 96-well plate where the

transfection media was replaced with media containing 10% dextran-charcoal-stripped serum in the presence or absence of 0, 0.1, 1, or 10 nmol/l synthetic androgen R1881 (Methyltrienolone, Sigma, St. Louis, MO). The Luciferase assays were performed at 48 hr post addition of R1881. All of the transfection assays were performed in triplicate and normalized to the cells untreated with R1881.

Western Blot

Cells were washed with PBS, pH 7.4, and lysed in Ripa lysis buffer (Sigma) supplemented with protease inhibitor cocktail (Roche, Indianapolis, IN). The cell lysate was incubated on ice for 30 min and was then centrifuged for 10 min at 4°C. Equal amounts of proteins were separated by SDS–PAGE and the resolved proteins were transferred to a PVDF membrane. After being blocked with 5% nonfat milk in PBS for 1 hr at room temperature, the blot was incubated with primary antibody overnight at 4°C. PSMA was detected using anti-PSMA (clone J591; kindly provided by Dr. Neil Bander, Weill Cornell Medical College, NY), AR was detected using anti-AR (clone SC816; Santa Cruz, Dallas, TX) and Actin was detected with anti-β-Actin (clone AC-15; Sigma). The membrane was then probed with anti-mouse secondary antibody (LI-COR, Lincoln, NE) conjugated with IRDye800CW for 1 hr and scanned on the Odyssey Infrared Imager (LI-COR) using the manufacturer's protocol.

In Vitro Growth Assay

Cells were plated in 96 well plates in either complete media or phenol red-free RPMI+10% charcoal stripped fetal bovine serum. Cell viability was quantified on days 0, 2, 4, 5, 6, and 7 by 3-(4, 5-dimethylthiazol-2-yl)-5-(3-carboxymethoxyphenyl)-2-(4-sulfophenyl)-2H-tetrazolium (MTS; Promega) according to the manufacturer's protocol. Data were normalized to day 0 and cell growth was represented in fold over starting.

In Vivo Studies

All studies were performed under Johns Hopkins University Animal Care and Use Committee-approved protocols. Four–seven week old intact male athymic nude mice (nu/nu; NCI, Frederick, MD and NCRNU-M; Taconic, Hudson, NY) were subcutaneously implanted with 2×10^6 cells (1:1, v:v with 50 μl of Matrigel® (Becton Dickson, Franklin Lakes, NJ) in Hank's Buffered Salt Solution; BD). After ∼10–14 days, 1 nmol of the PSMA specific fluorescent probe, YC27 [28] (LI-COR) was injected intraperitoneally (I.P.) and images were acquired at a post-injection (p.i.) time point of 24 hr using a Pearl Impulse Imager (LI-COR). Images are displayed using a pseudocolor output. All images are normalized to the same exposure time for each channel. In vivo imaging was performed using 2–2.5% isoflurane in oxygen inhalational anesthesia flowing at 2l/min on a 37°C bed. Ex vivo imaging was performed following anesthetized cervical dislocation.

For the androgen ablation studies, mice were surgically castrated 20 days after subcutaneous tumor cell implantation. Tumors were measured using calipers three times per week and volumes were calculated using the equation: (L × Wˆ2)/2 = V.

Histopathology and Immunofluorescence

Excised tumors and enlarged lymph nodes were divided into portions and either frozen on dry ice without embedding in OCT and stored at −80°C or were fresh-fixed in neutral-buffered formalin (Sigma). The frozen tissues were sectioned to 20 μm thicknesses using a Microm® HM 550 cryotome (Thermo Scientific, Walldorf, Germany) and annealed onto charged glass slides. Frozen sections for immunofluorescence were equilibrated to room temperature for 3 min and incubated twice in PBS for 5 min. The sections were then probed simultaneously for 1 hr at ambient temperature with mouse anti-human PSMA (Abcam, Cambridge, MA; clone GPC-05, ab66912) and rat anti-mouse CD31 conjugated to PE (Abcam; clone 390, ab25644; both used at 14 μg/ml) in PBS, pH 7.5 containing 10% fetal bovine serum (FBS; Gibco, Grand Island, NY). Slides were then washed twice in PBS for 5 min and probed with anti-mouse-FITC secondary antibody (Abcam; 1:200) for 30 min at ambient temperature. Slides were then incubated with Hoechst 33342 dye for 1.5 min (Invitrogen; 1:1,000 in PBS) to visualize nuclei and subsequently washed twice in PBS for 5 min followed by mounting with aqueous mounting media (Dako, Carpenteria, CA) and a glass cover slip. The dyes were excited by a Nikon Intensilight C-HGFI lamp and viewed using a Nikon 80i upright fluorescence microscope (Nikon, Melville, NY) equipped with a Nikon DS-Qi1Mc darkfield CCD camera and images were processed using the Nikon Elements Imaging Software. H&E stains were performed on formalin-fixed sections (4 μm) as per routine manufacturer's protocol (BBC Biochemical, Washington, DC) on a separate portion of the collected tissues.

Statistical Analysis

Standard unpaired two-tailed t-tests were performed using Microsoft Excel (Redmond, WA) with a *P*-value of less than 0.05 deemed as statistically significant.

Results

Genetic Confirmation of LNCaP Origin

In order to confirm that JHU-LNCaP-SM cells are of LNCaP origin and do not contain a contaminant from an unrelated cell line, we performed STR analysis as well as genomic DNA sequencing of a well characterized mutation in the AR of LNCaP cells (Codon 877: ACT->GCT, Thr->Ala). STR data were analyzed using the DSMZ database (http://www.dsmz.de/home.html), which confirmed that the STR profile of HP LNCaP was similar to LNCaP, having 83% profile similarity (Table I). The ATCC consortium suggests cells that share 75% or higher similarity are considered to be authentic [29]. In the STR analysis, the JHU-LNCaP-SM chromosomal pair 23 was found to be X, X instead of X, Y which represents partial loss of the Y chromosome and is common in immortalized cell lines [30] and is associated with increased risk of cancer in males [31]. As a secondary confirmation of origin, the region around codon 877 of the AR was sequenced from LNCaP, C4-2, and JHU-LNCaP-SM genomic DNA to confirm the presence of an AR point mutation. All cell lines contained the characteristic T877A mutation (Fig. 1). This mutation has also been found to be present in patient samples with advanced prostate cancer [30]. Additionally, scrutiny of a Western blot performed using cells cultured in both complete and charcoal-stripped media revealed the absence of the 75 kDa AR-v7 variant of AR in LNCaP, C4-2, and JHU-LNCaP-

SM (Fig. S5) whereas all three displayed the 120 kDa full length protein. Collectively, these data support that JHU-LNCaP-SM cells were derived from LNCaP cells and are similar to, but distinct from, C4-2 cells.

Androgen Dependence, Sensitivity, and PSMA Cellular Expression

To determine the growth rates of JHU-LNCaP-SM, relative to LNCaP and C4-2, cells were plated at equal density in multiple 96- well plates either in standard growth media containing 10% FBS or under androgen-deprived conditions in phenol red free RPMI 1640 containing 10% charcoal stripped FBS. Both C4-2 and JHU-LNCaP-SM had substantially faster growth rates than LNCaP under standard growth conditions (Fig. 2A). In the absence of androgens, the androgen-dependent LNCaP parental cells failed to grow, whereas C4-2 and JHU-LNCaP-SM continued to grow in the absence of androgens.

To determine the expression of total PSMA in LNCaP, C4-2, and JHU-LNCaP-SM cells, western blot analysis was performed in cells cultured in either complete media or androgen deprived media (Fig. 2B). PSMA expression in JHU-LNCaP-SM cells was found to be 15-fold lower than that of its parental cell line and 5-fold lower than C4-2 when cells were cultured in complete media. AR expression in JHU-LNCaP-SM and C4-2 cells was slightly reduced in complete media compared to LNCaP cells. Under androgen deprived conditions, PSMA expression uniformly increased by 2–3 fold in all cell lines when compared to cells cultured in media containing complete FBS. AR expression in JHU-LNCaP-SM cells was lower in total expression in charcoal stripped media when compared to both LNCaP and C4-2 cells (Fig. 2B).

To further study the responsiveness of JHU-LNCaP-SM cells to androgen stimulation, cells were transfected with an AR-responsive luciferase reporter [32] and stimulated with 0.1, 1.0, or 10nM of the synthetic androgen R1881 for 48 hr. LNCaP and C4-2 cells experienced significantly elevated luciferase expression at all concentrations of R1881, whereas JHU-LNCaP-SM cells only show a modest increase with R1881 stimulation (Fig. 3). Cell culture media from each well was harvested prior to luciferase assay to measure secreted PSA. PSA levels in all cell lines increased with addition of R1881 and were higher in the androgen insensitive C4-2 cells in comparison with LNCaP In contrast, PSA levels in JHU-LNCaP-SM were much lower than in both LNCaP and C4-2 cells.

Tumorigenicity of JHU-LNCaP-SM in Immunocompromized Mice

Subcutaneously inoculated JHU-LNCaP-SM cells grew rapidly into tumors in intact male athymic nude mice with a 100% (13/13) tumor take rate. Tumors were palpable as early as 5 days post inoculation, whereas animals similarly inoculated with parental LNCaP cells were unable to form tumors (0/15; Fig. 4A) over the same time period. To further evaluate the androgen independence of JHU-LNCaP-SM tumor xenografts, mice bearing $\sim$300 mm^3 established tumors were surgically castrated. Both treated and untreated groups displayed exponential growth and had comparable final tumor volumes, demonstrating growth insensitivity to androgen (Fig. 4B).

Hemorrhagic Phenotype of Jhu-LNCaP-SM Xenografts

All JHU-LNCaP-SM tumor xenografts larger than 4mm in diameter displayed a characteristic spreading hemorrhagic phenotype within and adjacent to the tumor parenchyma. Mice with xenografts reaching 1 cm in diameter displayed hemorrhage spreading as far away as 2 cm from the tumor along the flank (Fig. 5A–C). This is in contrast to the appearance of xenografts from parental LNCaP or C4-2 (Fig. 6H), which are also hemorrhagic although hemorrhage is confined within the tumor. Unlike in LNCaP and C4-2 tumor xenografts, hemorrhage patterns within the JHU-LNCaP-SM tumors were macroscopically heterogeneous and characteristically displayed a grossly marbled appearance of red and white tissue. H&E analysis of the tumor parenchyma confirmed positive tumor histology throughout the xenografts as well as abundant extravascular red blood cells (Fig. 5D).

PSMA Expression in JHU-LNCaP-SM Xenografts

Macroscopic primary tumor PSMA expression patterns and scrutiny for PSMA-positive metastases were undertaken among mice bearing C4-2 and JHU-LNCaP-SM tumor xenografts. PSMA was detected in vivo and ex vivo using near IR fluorescence imaging. Both tumor types avidly retained the targeted optical probe (Fig. 6A–G). Ex vivo imaging of dissected mice revealed that the tumor parenchyma of JHU-LNCaP-SM and C4-2 xenografts expressed PSMA in a heterogeneous manner (Fig. 6B–G).

Immunofluorescence staining for PSMA expression in xenografts from LNCaP, C4-2, and JHU-LNCaP-SM showed that PSMA spatial expression within LNCaP xenograft epithelium is nearly homogeneous throughout tumor sections (Fig. 7A and supplementary Fig. S1) whereas PSMA distribution in both C4-2 and JHU-LNCaP-SM tumor sections is heterogeneous and largely co-localized to peri-vascular epithelium (Fig. 7B–C and Suppl. Fig. S2 and S3).

PSMA-expressing lymph node metastases were observed in 100% (13/13) of mice bearing subcutaneous xenografts that had reached 1cm in diameter (Fig. 8A–C and Suppl. Fig. S4). Metastases were both local and distant from the site of the primary tumor and included axillary, brachial, cervical, mediastinal, inguinal, renal, and lumbar nodes with proximal axillary nodes being most frequently positive. Immunofluorescence and H & E histology confirmed YC27 positive nodes to contain tumor cells (Fig. 8D–H). No macroscopic non-lymphoid or bony metastases were observed during the period of study due to primary tumor overgrowth, re-growth (after primary tumor resection, n = 10 mice) or cost of long-term housing while waiting for bony or other soft tissue growth. It should be noted that resections must be performed in small primary tumors (<5 mm) to prevent lethal hemorrhage, which seem to precede/preclude metastasis.

Discussion

Herein we have reported a new LNCaP cell line derivative, JHU-LNCaP-SM. These cells are of LNCaP origin and were generated by long term passage in typical cell culture conditions. The JH-LNCaP-SM cells retain expression of the parental mutated AR gene,

although unlike LNCaP, are not dependent upon androgens for growth. JHU-LNCaP-SM retains androgen-sensitive PSA and PSMA expression, exhibits diminished AR expression upon androgen ablation and has lost a portion of its Y chromosome. These cells are able to form subcutaneous tumors very quickly, contrasted with the current parental LNCaP line and reliably microscopically and macroscopically metastasize to lymph nodes within 2–3 weeks of implantation, unlike the C4-2 derivative. The reliable metastatic phenotype of this model, from subcutaneous to lymph node, makes it more suitable to study longitudinal spontaneous metastatic disease than some other metastatic models, such as orthotopic xenografts and autochthonous transgenic models, which either perish from the primary tumor burden prior to assayable metastatic events or do not express PSMA, an important feature of clinical disease.

The JH-LNCaP-SM xenografts display a striking subcutaneous hemorrhagic phenotype extending well beyond the tumor parenchyma. This broad hemorrhagic characteristic of JHU-LNCaP-SM xenografts may contribute to their increased metastatic phenotype. An unexplored possibility is a deficiency in pericytes, the cells that line vasculature-associated endothelial cells, which can cause hemorrhage and vasculature leakiness. It has been shown that this deficiency correlates to increased metastases in both animal models [33] and humans [34]. Another LNCaP subline, LNCaP-19 with fewer pericytes than the parental cell line was shown to have increased invasiveness in vitro, increased vasculature density and accelerated growth relative to LNCaP in mouse xenograft models [35,36]. Investigation of pericyte densities and vascular integrity in JHU-LNCaP-SM xenografts sections should be undertaken to investigate this possibility.

PSMA expression patterns in both JHU-LNCaP-SM and C4-2 xenografts were macroscopically and microscopically heterogeneous in distribution. Microscopic examination revealed that PSMA expression in both C4-2 and JHU-LNCaP-SM tumor sections was found to be enriched in peri-vascular regions. This pattern is also observed in LNCaP xenograft sections although LNCaP tumors also abundantly express PSMA in epithelium distant from vascular beds (Fig. 7A and B and Fig. S1). High-passage derivatives like C4-2 and JHU-LNCaP-SM and even high passaged parental LNCaP spontaneously decrease PSMA expression over time, although PSMA becomes more enzymatically active [37]. Primary clinical specimens of prostate cancer exhibit PSMA expression within and then spreading outwards from secretory glands with increasing Gleason score. The expression patterns within prostate cancer metastases are similar with glandular or microglandular differentiation and PSMA expression becomes highly heterogeneous in more anaplastic lesions [38]. PSMA expression has even been reported to induce the expression and release of cytokines and chemokines, such as IL6 and CCL5, which influence both angiogenesis and metastasis [39]. Tumor xenografts resemble high grade, anaplastic tumors and JHU-LNCaP-SM tumors and related lines may provide an excellent opportunity to study the effects of PSMA expression on both vascular and metastatic biological behaviors.

Conclusion

The JHU-LNCaP-SM model is a valuable addition to the prostate cancer cell line repertoire and its advantage over C4-2 is reliable spontaneous spread from subcutaneous xenografts

into lymph nodes, making it a useful model to study prostate cancer metastasis and to test experimental diagnostics and therapies for the treatment of advanced prostate cancer.

Supplementary Material

Refer to Web version on PubMed Central for supplementary material.

Acknowledgments

We would like to acknowledge Mrudulla Pullumbhatla for culturing the C4-2 cells for implantation into mice and Sam Denmeade for his kind gift of a primary LNCaP xenograft tumor sample. We would also like to acknowledge funding through NIH grants CA134675, CA184228, CA183031, and EB005324.

Grant sponsor: NIH; Grant numbers: CA134675; CA184228; CA183031; EB005324.

References

1. Horoszewicz JS, Leong SS, Kawinski E, Karr JP, Rosenthal H, Chu TM, Mirand EA, Murphy GP. LNCaP model of human prostatic carcinoma. Cancer Res. 1983; 43(4):1809–1818. [PubMed: 6831420]
2. Lim DJ, Liu XL, Sutkowski DM, Braun EJ, Lee C, Kozlowski JM. Growth of an androgen-sensitive human prostate cancer cell line, LNCaP, in nude mice. Prostate. 1993; 22(22):109–118. [PubMed: 7681204]
3. Culig Z, Hoffmann J, Erdel M, Eder EI, Hobisch A, Hittmair A, Bartsch G, Utermann G, Schneider MR, Parczyk K, Klocker H. Switch from antagonist to agonist of the androgen receptor bicalutamide is associated with prostate tumour progression in a new model system. Br J Cancer. 1999; 81(2):242–251. [PubMed: 10496349]
4. Gao M, Ossowski L, Ferrari AC. Activation of Rb and decline in androgen receptor protein precede retinoic acid-induced apoptosis in androgen-dependent LNCaP cells and their androgen-independent derivative. J Cell Physiol. 1999; 179(3):336–346. [PubMed: 10228952]
5. Kokontis JM, Hay N, Liao S. Progression of LNCaP prostate tumor cells during androgen deprivation: hormone-independent growth, repression of proliferation by androgen, and role for p27Kip1 in androgen-induced cell cycle arrest. Mol Endocrinol. 1998; 12(7):941–953. [PubMed: 9658399]
6. Lu S, TsaiS Y, Tsai MJ. Molecular mechanisms of androgen-independent growth of human prostate cancer LNCaP-AI cells. Endocrinology. 1999; 140(11):5054–5059. [PubMed: 10537131]
7. Thalmann GN, Sikes RA, Wu TT, Degeorges A, Chang SM, Ozen M, Pathak S, Chung LW. LNCaP progression model of human prostate cancer: Androgen-independence and osseous metastasis. Prostate. 2000; 44(2):91–103. [PubMed: 10881018]
8. van Steenbrugge GJ, van Uffelen CJ, Bolt J, Schroder FH. The human prostatic cancer cell line LNCaP and its derived sublines: An in vitro model for the study of androgen sensitivity. J Steroid Biochem Mol Biol. 1991; 40(1–3):207–214. [PubMed: 1958522]
9. Denmeade SR, Sokoll LJ, Dalrymple S, Rosen DM, Gady AM, Bruzek D, Ricklis RM, Isaacs JT. Dissociation between androgen responsiveness for malignant growth vs. expression of prostate specific differentiation markers PSA, hK2, and PSMA in human prostate cancer models. Prostate. 2003; 54(4):249–257. [PubMed: 12539223]
10. Igawa T, Lin FF, Lee MS, Karan D, Batra SK, Lin MF. Establishment and characterization of androgen-independent human prostate cancer LNCaP cell model. Prostate. 2002; 50(4):222–235. [PubMed: 11870800]
11. Abate-Shen C, Shen MM. Mouse models of prostate carcinogenesis. Trends in Genetics. 2002; 18(5):S1–S5. [PubMed: 12047956]
12. Valkenburg KC, Pienta KJ. Drug discovery in prostate cancer mouse models. Expert Opin Drug Discov. 2015; 10(9):1011–1024. [PubMed: 26027638]

13. Sato N, Gleave ME, Bruchovsky N, Rennie PS, Beraldi E, Sullivan LD. A metastatic and androgen-sensitive human prostate cancer model using intraprostatic inoculation of LNCaP cells in SCID mice. Cancer Res. 1997; 57(8):1584–1589. [PubMed: 9108464]
14. Silver DA, Pellicer I, Fair WR, Heston WD, Cordon-Cardo C. Prostate-specific membrane antigen expression in normal and malignant human tissues. Clin Cancer Res. 1997; 3(1):81–85. [PubMed: 9815541]
15. Perner S, Hofer MD, Kim R, Shah RB, Li H, Mo€ller P, Hautmann RE, Gschwend JE, Kuefer R, Rubin MA. Prostate-specific membrane antigen expression as a predictor of prostate cancer progression. Hum Pathol. 2007; 38(5):696–701. [PubMed: 17320151]
16. Foss CA, Mease RC, Cho SY, Kim HJ, Pomper MG. GCPII imaging and cancer. Curr Med Chem. 2012; 19(9):1346–1359. [PubMed: 22304713]
17. Bander NH, Milowsky MI, Nanus DM, Kostakoglu L, Vallabhajosula S, Goldsmith SJ. Phase I trial of 177lutetium-labeled J591, a monoclonal antibody to prostate-specific membrane antigen, in patients with androgen-independent prostate cancer. J Clin Oncol. 2005; 23(21):4591–4601. [PubMed: 15837970]
18. Banerjee SR, Foss CA, Castanares M, Mease RC, Byun Y, Fox JJ, Hilton J, Lupold SE, Kozikowski AP, Pomper MG. Synthesis and evaluation of technetium-99m- and rhenium-labeled inhibitors of the prostate-specific membrane antigen (PSMA). J Med Chem. 2008; 51(15):4504–4517. [PubMed: 18637669]
19. Chen Y, Foss CA, Byun Y, Nimmagadda S, Pullambhatla M, Fox JJ, Castanares M, Lupold SE, Babich JW, Mease RC, Pomper MG. Radiohalogenated prostate-specific membrane antigen (PSMA)-based ureas as imaging agents for prostate cancer. J Med Chem. 2008; 51(24):7933–7943. [PubMed: 19053825]
20. Dassie JP, Liu XY, Thomas GS, Whitaker RM, Thiel KW, Stockdale KR, Meyerholz DK, McCaffrey AP, McNamara JO, Giangrande PH. Systemic administration of optimized aptamer-siRNA chimeras promotes regression of PSMA-expressing tumors. Nat Biotechnol. 2009; 27(9):839–849. [PubMed: 19701187]
21. Farokhzad OC, Cheng J, Teply BA, Sherifi I, Jon S, Kantoff PW, Richie JP, Langer R. Targeted nanoparticle-aptamer bioconjugates for cancer chemotherapy in vivo. Proc Natl Acad Sci USA. 2006; 103(16):6315–6320. [PubMed: 16606824]
22. Morris MJ, Divgi CR, Pandit-Taskar N, Batraki M, Warren N, Nacca A, Smith-Jones P, Schwartz L, Kelly WK, Slovin S, Solit D, Halpern J, Delacruz A, Curley T, Finn R, O'Donoghue JA, Livingston P, Larson S, Scher HI. Pilot trial of unlabeled and indium-111-labeled anti-prostate-specific membrane antigen antibody J591 for castrate metastatic prostate cancer. Clin Cancer Res. 2005; 11(20):7454–7461. [PubMed: 16243819]
23. Nakajima T, Mitsunaga M, Bander NH, Heston WD, Choyke PL, Kobayashi H. Targeted, activatable, in vivo fluorescence imaging of prostate-specific membrane antigen (PSMA) positive tumors using the quenched humanized J591 antibody-indocyanine green (ICG) conjugate. Bioconjug Chem. 22(8):1700–1705. [PubMed: 21740058]
24. Ni X, Zhang Y, Ribas J, Chowdhury WH, Castanares M, Zhang Z, Laiho M, DeWeese TL, Lupold SE. Prostate-targeted radiosensitization via aptamer-shRNA chimeras in human tumor xenografts. J Clin Invest. 121(6):2383–2390. [PubMed: 21555850]
25. Banerjee SR, Pullambhatla M, Byun Y, Nimmagadda S, Foss CA, Green G, Fox JJ, Lupold SE, Mease RC, Pomper MG. Sequential SPECT and optical imaging of experimental models of prostate cancer with a dual modality inhibitor of the prostate-specific membrane antigen. Angew Chem Int Ed Engl. 2011; 50(39):9167–9170. [PubMed: 21861274]
26. Wright GL Jr, Haley C, Beckett ML, Schellhammer PF. Expression of prostate-specific membrane antigen in normal, benign, and malignant prostate tissues. Urol Oncol. 1995; 1(1):18–28. [PubMed: 21224086]
27. Lubahn DB, Brown TR, Simental JA, Higgs HN, Migeon CJ, Wilson EM, French FS. Sequence of the intron/exon junctions of the coding region of the human androgen receptor gene and identification of a point mutation in a family with complete androgen insensitivity. Proc Natl Acad Sci USA. 1989; 86(23):9534–9538. [PubMed: 2594783]

28. Chen Y, Dhara S, Banerjee SR, Byun Y, Pullambhatla M, Mease RC, Pomper MG. A low molecular weight PSMA-based fluorescent imaging agent for cancer. Biochem and Biophys Res Commun. 2009; 390(3):624–629. [PubMed: 19818734]
29. Katsnelson A. Biologists tackle cells' identity crisis. Nature. 2010; 465(7298):537. [PubMed: 20520682]
30. Gaddipati JP, McLeod DG, Heidenberg HB, Sesterhenn IA, Finger MJ, Moul JW, Srivastava S. Frequent detection of codon 877 mutation in the androgen receptor gene in advanced prostate cancers. Cancer Res. 1994; 54(11):2861–2864. [PubMed: 8187068]
31. Wright GL Jr, Grob BM, Haley C, Grossman K, Newhall K, Petrylak D, Troyer J, Konchuba A, Schellhammer PF, Moriarty R. Upregulation of prostate-specific membrane antigen after androgen-deprivation therapy. Urology. 1996; 48(2):326–334. [PubMed: 8753752]
32. Hoti N, Li Y, Chen CL, Chowdhury WH, Johns DC, Xia Q, Kabul A, Hsieh JT, Berg M, Ketner G, Lupold SE, Rodriguez R. Androgen receptor attenuation of Ad5 replication: Implications for the development of conditionally replication competent adenoviruses. Mol Ther. 2007; 15(8):1495–1503. [PubMed: 17565351]
33. Xian X, Håkansson J, Ståhlberg A, Lindblom P, Betsholtz C, Gerhardt H, Semb H. Pericytes limit tumor cell metastasis. J Clin Invest. 2006; 116(3):642–651. [PubMed: 16470244]
34. Yonenaga Y, Mori A, Onodera H, Yasuda S, Oe H, Fujimoto A, Tachibana T, Imamura M. Absence of smooth muscle actin-positive pericyte coverage of tumor vessels correlates with hematogenous metastasis and prognosis of colorectal cancer patients. Oncology. 2005; 69(2):159–166. [PubMed: 16127287]
35. Welen K, Jennbacken K, Tesan T, Damber JE. Pericyte coverage decreases invasion of tumour cells into blood vessels in prostate cancer xenografts. Prostate Cancer Prostatic Dis. 2008; 12(1): 41–46. [PubMed: 18521102]
36. Gustavsson H, Welén K, Damber JE. Transition of an androgen-dependent human prostate cancer cell line into an androgen-independent subline is associated with increased angiogenesis. Prostate. 2005; 62(4):364–373. [PubMed: 15389782]
37. Denmeade SR, Sokoll LJ, Dalrymple S, Rosen DM, Gady AM, Bruzek D, Ricklis RM, Isaacs JT. Dissociation between androgen responsiveness for malignant growth vs. expression of prostate specific differentiation markers PSA, hK2, and PSMA in human prostate cancer models. Prostate. 2003; 54(4):249–257. [PubMed: 12539223]
38. Mannweiler S, Amersdorfer P, Trajanoski S, Terrett J, King D, Mehes G. Heterogeneity of Prostate-Specific Membrane Antigen (PSMA) expression in prostate carcinoma with distant metastasis. Pathol Oncol Res. 2009; 15(2):167–172. [PubMed: 18802790]
39. Colombatti M, Grasso S, Porzia A, Fracasso G, Scupoli MT, Cingarlini S, Poffe O, Naim HY, Heine M, Tridente G, Mainiero F, Ramarli D. The Prostate Specific Membrane Antigen regulates the expression of IL-6 and CCL5 in prostate tumour cells by activating the MAPK pathways(1). PLoS ONE. 2009; 4(2):e4608. [PubMed: 19242540]

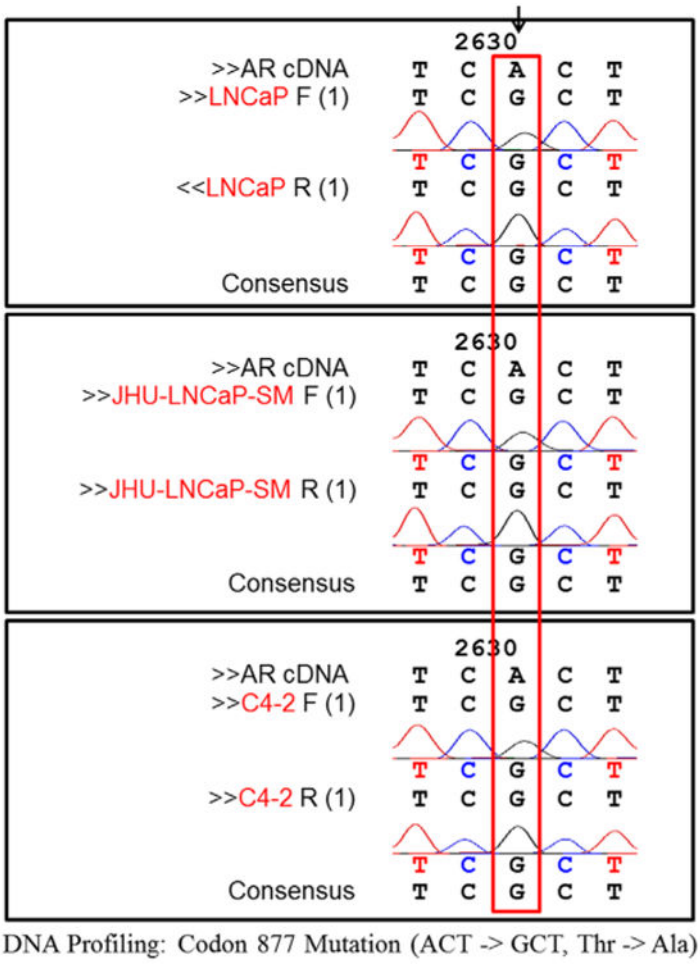

Fig. 1.

Genetic confirmation of LNCaP origin by DNA sequencing. To determine the origin of the JHU-LNCaP-SM cell line, genomic DNA sequencing analysis was performed on segments with known LNCaP AR mutations. The sequencing showed that the LNCaP, JHU-LNCaP-SM, and C4-2 lines all contained the LNCaP specific AR mutation (ACT–GCT).

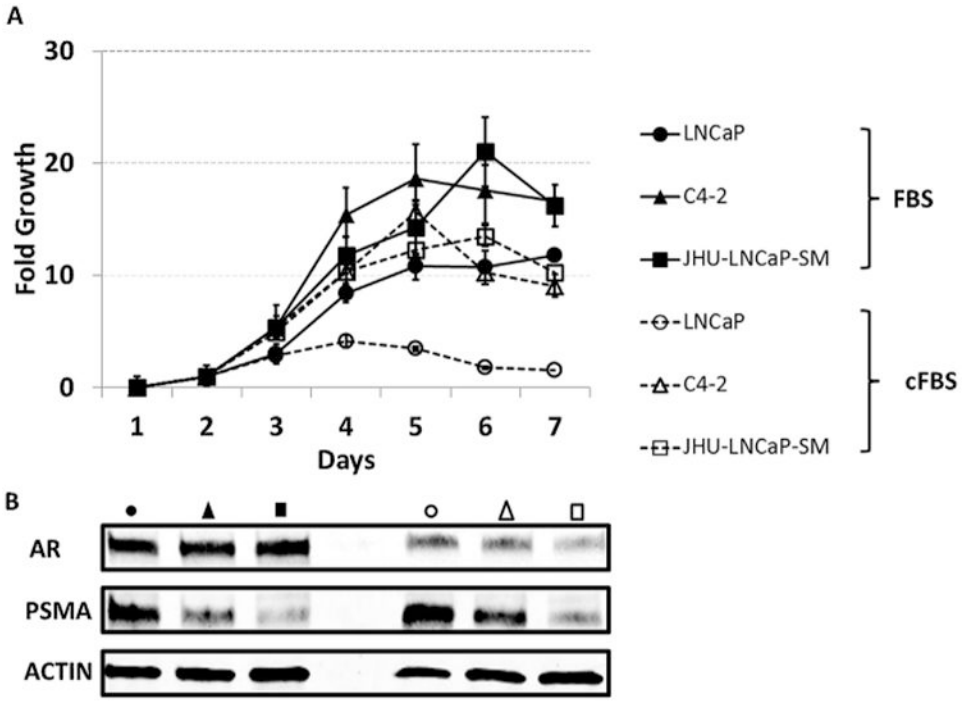

Fig. 2.

Relative growth rates and protein expression of AR and PSMA of LNCaP cells and derivatives in full and charcoal-stripped media culture conditions. (**A**) Growth rates of the LNCaP, JHU-LNCaP-SM, and C4-2 cell lines were determined by plating out equal densities in 96 well plates and following growth by MTS assay. To determine if the in vitro growth of the cell lines was androgen sensitive they were also cultured in normal or charcoal stripped serum conditions and followed as previous. (**B**) Lysates were taken of cell pellets from the LNCaP, JHU-LNCaP, and C4-2 cell lines grown in either normal or charcoal stripped serum media and western blot was used to determine relative AR and PSMA protein expression.

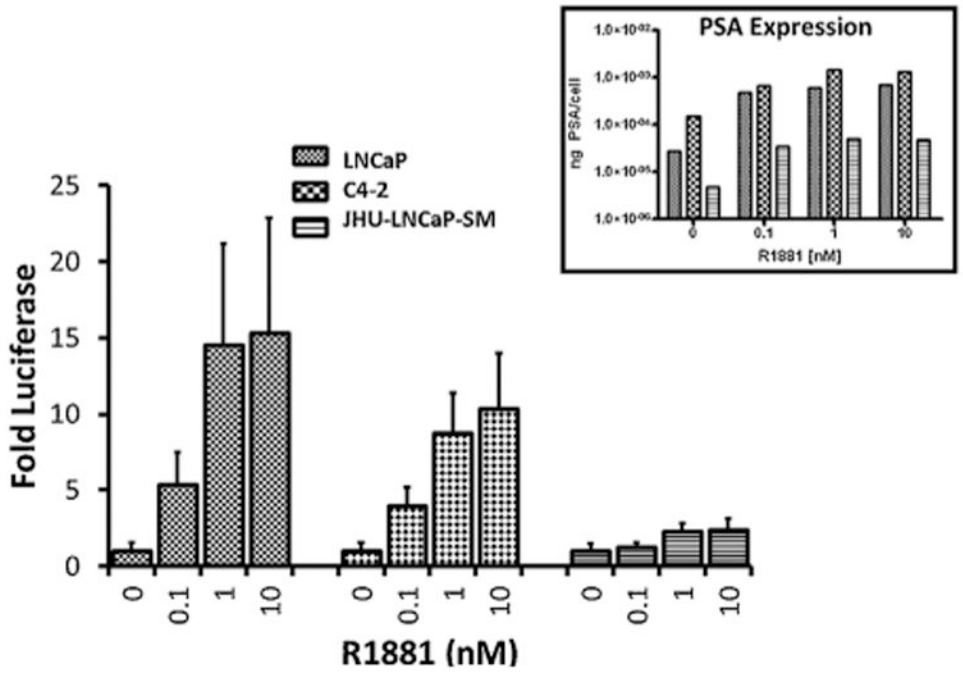

Fig. 3.

Androgen receptor activity in cell culture. To determine if the cell lines were androgen sensitive a luciferase reporter assay was conducted on the LNCaP, JHU-LNCaP-SM, and C4-2 cell lines. All lines were stimulated with increasing titrations of the synthetic androgen (R1881) in cell culture and monitored by an androgen dependent promoter luciferase activity. n = 8; all concentrations for all cell lines had a *P*-value of <0.05 compared to the 0nM R1881 using the standard unpaired *t*-test except for 0 nM R1881 compared to 0.1 nM R1881 for JHU-LNCaP-SM. PSA expression levels were also determined for each cell line with androgen stimulation (insert).

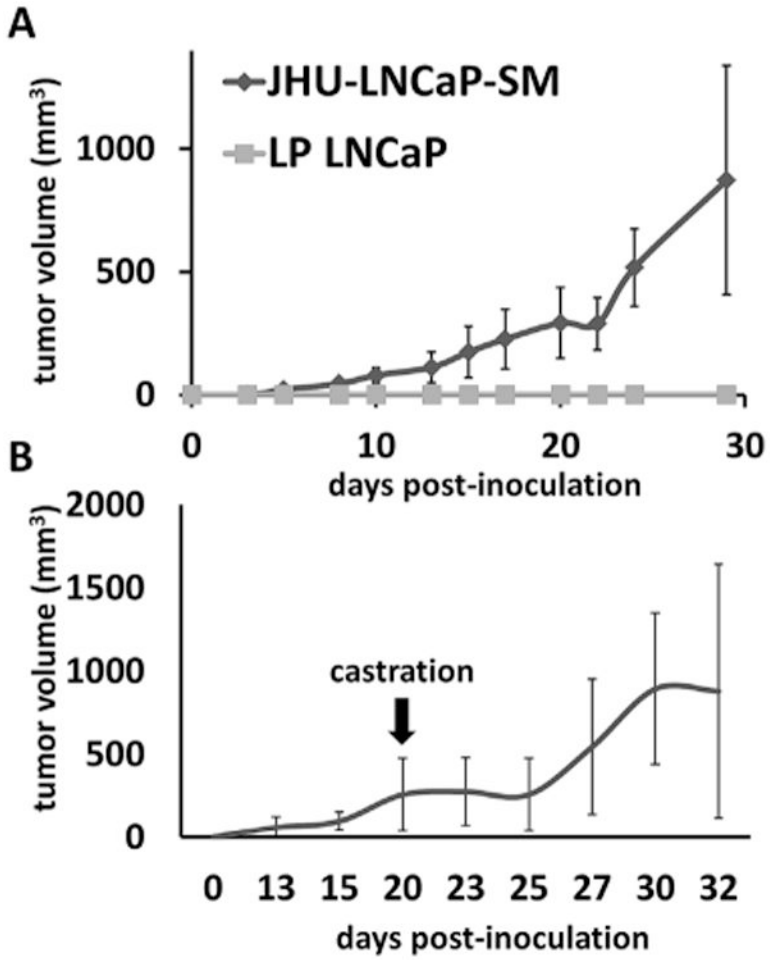

Fig. 4.

Xenograft growth rate in male athymic nude mice. (**A**) JHU-LNCaP-SM and LNCaP cells (2×10^6) were injected subcutaneously in 6 week old male athymic nude mice and volume measurements were taken over a 30 day period. (**B**) A cohort of the JHU-LNCaP-SM xenograft animals were castrated to determine if the xenografts were androgen sensitive in vivo.

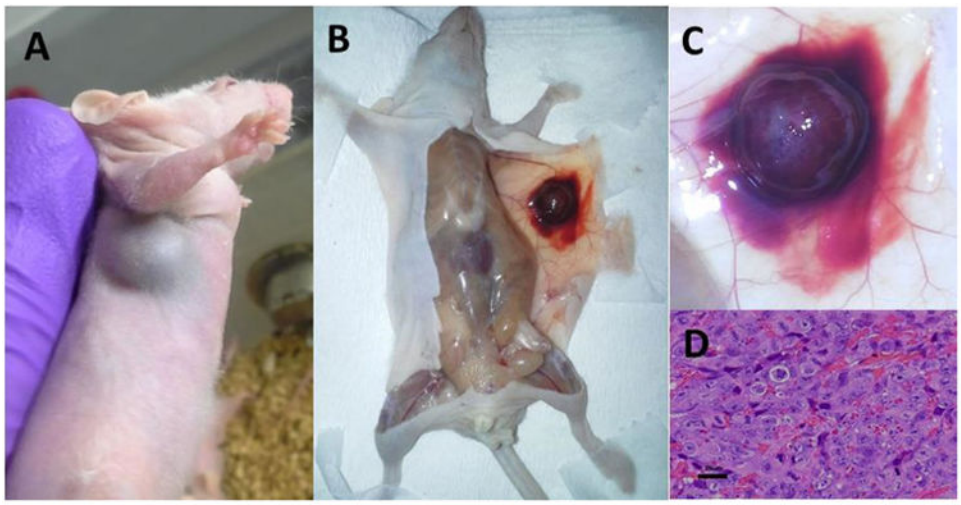

Fig. 5.

In vivo and ex vivo characterization of JHU-LNCaP-SM xenografts. (**A–C**) Macroscopic characterization of primary tumors from JHU-LNCaP-SM xenografts revealed a consistently hemorrhagic appearance in vivo and ex vivo. (**D**) H&E staining of xenograft sections confirmed tumor presence and hemorrhagic phenotype.

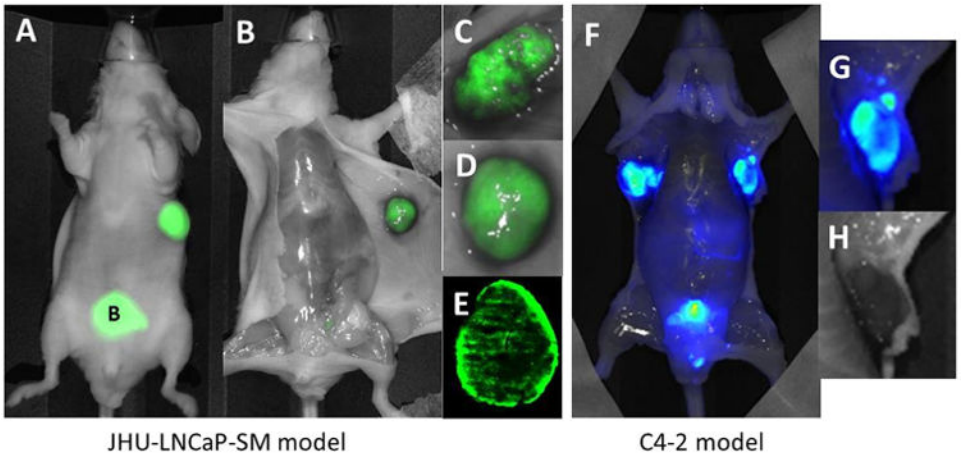

Fig. 6.

In vivo and ex vivo imaging of PSMA expression in JHU-LNCaP-SM and C4-2 xenografts. (**A**) Optical imaging of PSMA using YC27 showed that tumors could easily be non-invasively delineated from normal tissue in vivo. (**B–D**) Probe excretion through the urinary bladder can also be seen, shown as “B.” (**E**) Tumor uptake of YC27 showing mottled PSMA distribution was confirmed ex vivo as well as in whole mount sections. (**F** and **G**) PSMA sparsely expressing C4-2 xenografts were also easily delineated by NIRF imaging in vivo and ex vivo. (**H**) C4-2 shows a hemorrhagic phenotype but without the peri-tumoral subcutaneous spread.

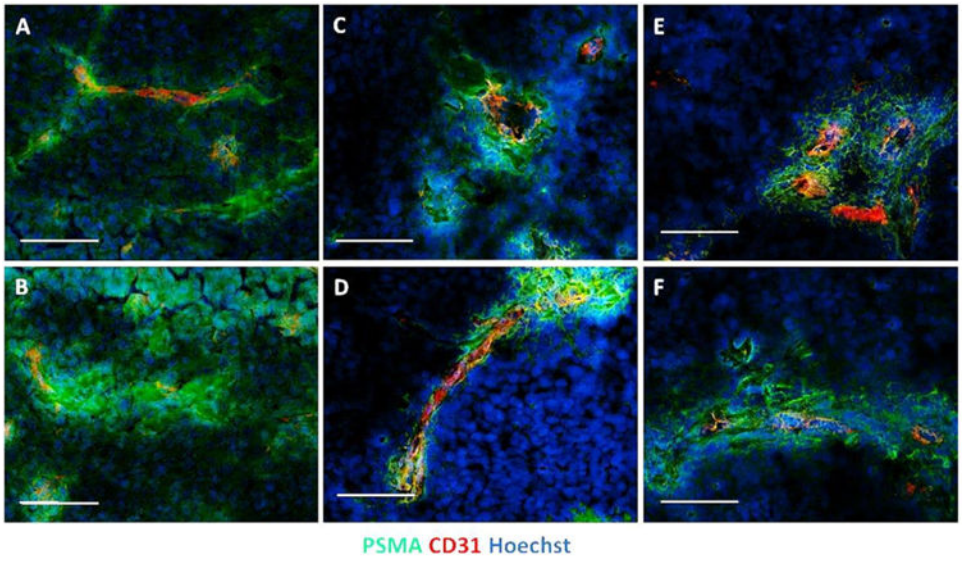

Fig. 7.

Proximal expression of PSMA in context with CD31 expression in LNCaP, JHU-LNCaP-SM, and C4-2 tumor xenografts. PSMA and CD31 expression patterns were determined using immunofluorescence microscopy upon primary tumor xenograft sections. (**A** and **B**) LNCaP tumors are represented, (**C** and **D**) represents JHU-LNCaP-SM tumors, and (**E** and **F**) depicts C4-2 xenograft tumors. Markers and channels are as indicated and are optimized for intensities individually. Scale bar = 100 μm.

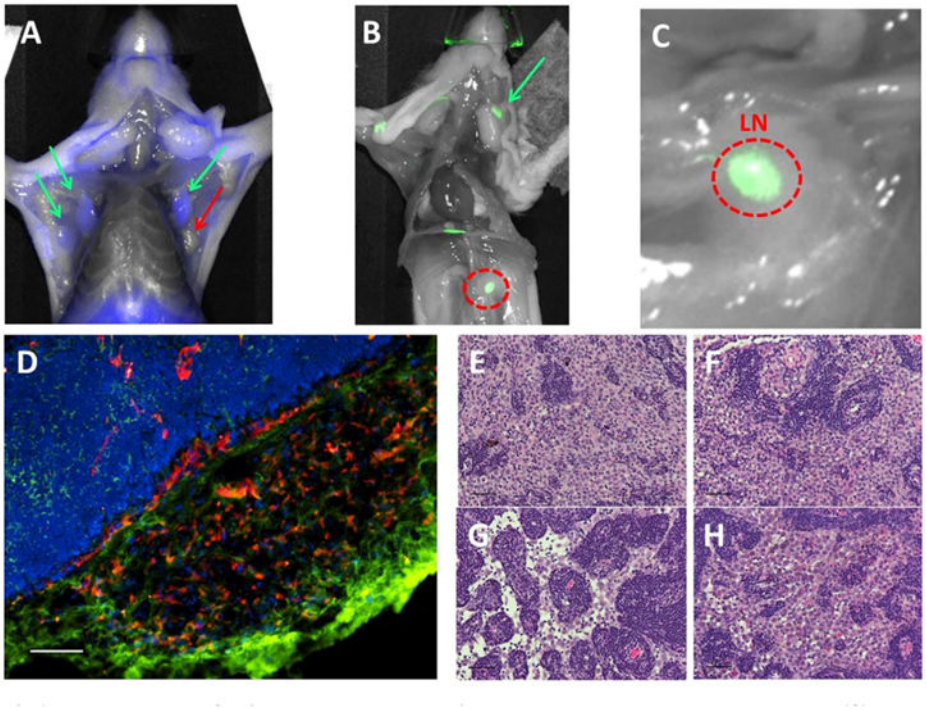

Fig. 8.

PSMA-expressing JHU-LNCaP-SM subcutaneous xenografts spontaneously metastasize to lymph nodes. (**A**) Ex vivo PSMA-targeted optical imaging of lymph nodes from selected mice that exhibited spontaneous metastasis from subcutaneous JHU-LNCaP-SM primary xenografts where green arrows show PSMA positive axillary lymph nodes and red is a negative node. (**B** and **C**) The red circle is a positive renal lymph node and also shown is a superficial cervical lymph node denoted by a green arrow. (**D**) Frozen sections of lymph node metastasis were analyzed by immunofluorescence for PSMA and CD31 expression and confirm the presence of PSMA-expressing cells within a vascular cage at the edge of packed lymphatic cells (scale bar = 100 μm). (**E–H**) H&E staining of various PSMA positive nodes confirming the presence of tumor cells (scale bar = 50μm).

Table I

Genetic Confirmation of LNCaP Origin by STR Analysis

	LNCaP reference (DSMZ database)	LNCaP	C4-2	JHU-LNCaP-SM
Amelogenin	X, Y	X, Y	X, Y	X, X
CSF1PO	10, 11	10, 11, 12	9, 10, 11, 12	9, 10, 11, 12
D13S317	10, 12	10, 11, 12	10, 11, 12	9, 11, 12, 13
D16S539	11, 11	11, 11	10, 11	10, 11
D5S818	11, 12	11, 12	11, 12	10, 11, 12, 13
D7S820	9.1, 10.3	9.1, 9.3, 10.3	9.1, 9.3, 10.3	9.1, 10.1, 10.2, 10.3
TH01	9, 9	9, 9	9, 9	9,9
TPOX	8, 9	8, 9	8, 9	9,9
vWA	16, 18	16, 18	16, 17, 18	15,16,17,18